SUPPORTING INFORMATION FOR:

Prion gene paralogs are dispensable for early zebrafish development but have non-additive roles in seizure susceptibility

Patricia L.A. Leighton, Richard Kanyo, Gavin Neil, Niall M. Pollock, and W. Ted Allison

Consisting of:
7 Supplemental Tables
13 Supplemental Figures

Supplementary Table S1. Primers used to engineer *prp1* TALENs

Assay	Primers
Colony PCR screening	**Forward primer:** **5'-AGT AAC AGC GGT AGA GGC AG-3'** **Reverse primer:** **5'-TTA ATT CAA TAT ATT CAT GAG GCA C-3'**
Sequencing	**Forward primer:** **5'-AGT AAC AGC GGT AGA GGC AG-3'** **Reverse primer 1:** **5'-ATT GGG CTA CGA TGG ACT CC-3'** **Reverse primer 2:** **5'-TTA ATT CAA TAT ATT CAT GAG GCA C-3'**

Supplementary Table S2. Primers for screening for TALEN mutations and genotyping *prp1* and *prp2* mutants

Assay	Gene	Primers
HRM Analysis	***prp1***	**Forward:** **5'-TGT TAG GAC CAA AAT GGG GGA G-3'** **Reverse:** **5'-GAA CAG TCT TGC TTA CAG TGC C-3'**
RFLP Analysis	***prp2***	**Forward:** **5'-TCC CCT GGA AAC TAT CCT CGC CAA C-3'** **Reverse:** **5'-TGGGTTAGAGCCTGCTGGTGG-3'**
Generate PCR Amplicon for Topo Cloning or Direct sequencing	***prp1***	**Forward:** **5'- AGC ATT CTC CAT TAG ACC TGT-3'** **Reverse** **5'-CTG CTG GTT AGG GTA GCC TG-3'**
	prp2	**Forward:** **5'-ATG GGT CGC TTA ACA ATA CTA TTG-3'** **Reverse:** **5'-CCA TTC ATG TTA CCG TCA GG-3'**

Supplementary Table S3. Gene-specific primers for characterizing *prp1* and *prp2* mutant transcripts by 5' RACE. Gene-specific regions of primers are underlined.

Assay	Gene	Primers
5'RACE	***prp1***	**5'-** GAT TAC GCC AAG CTT AGC GTT CCT CCT GTG GGC TTC TGA ACT G **-3'**
	prp2	**5'-** GAT TAC GCC AAG CTT GGT TGG CTG GGT GTT TCT GGT GGG TTT G **-3'**

Supplemental Table S4. Data plotted in Figure 4E regarding number of neuromasts in various prion mutants. Values in table represent the number of larvae that had that particular abundance of neuromasts.

	Number neuromasts						Total
	2	**3**	**4**	**5**	**6**	**7**	**larvae**
wildtype		2	20	30	2		54
prp2$^{ua5001/ua5001}$				7	19		26
prp1$^{ua5004/ua5004}$		3	7				10
prp1$^{ua5003/ua5003}$	1	4	7	12	1		25
prp1$^{+/ua5004}$; *prp2*$^{+/ua5001}$			2	10			12
prp1$^{ua5003/ua5003}$; *prp2*$^{ua5001/ua5001}$	1			11	7		19

Supplemental Table S5. Data plotted in Supplemental Figure S12B regarding number of neuromasts in various prion mutants. Values in table represent the number of larvae that had that particular abundance of neuromasts.

	Number neuromasts						Total
	2	**3**	**4**	**5**	**6**	**7**	**larvae**
wildtype			7	10	1		18
prp1$^{ua5004/ua5004}$	3	5	7	3	1		21

Supplemental Table S6. Data plotted in Supplemental Figure S12C regarding number of neuromasts in various prion mutants. Values in table represent the number of larvae that had that particular abundance of neuromasts.

	Number neuromasts							Total
	2	**3**	**4**	**5**	**6**	**7**	**8**	**larvae**
wildtype				8	71	32	5	116
prp1$^{+/ua5004}$			2	13	5	2		22
prp1$^{ua5004/ua5004}$	1		3	20	9	1		34

Supplemental Table S7. Data plotted in Supplemental Figure S12D regarding number of neuromasts in various prion mutants. Values in table represent the number of larvae that had that particular abundance of neuromasts.

	Number neuromasts							Total
	2	**3**	**4**	**5**	**6**	**7**	**8**	**larvae**
wildtype	1	1	15	48	13	1		79
prp2$^{ua5001/ua5001}$				25	33	9	2	69

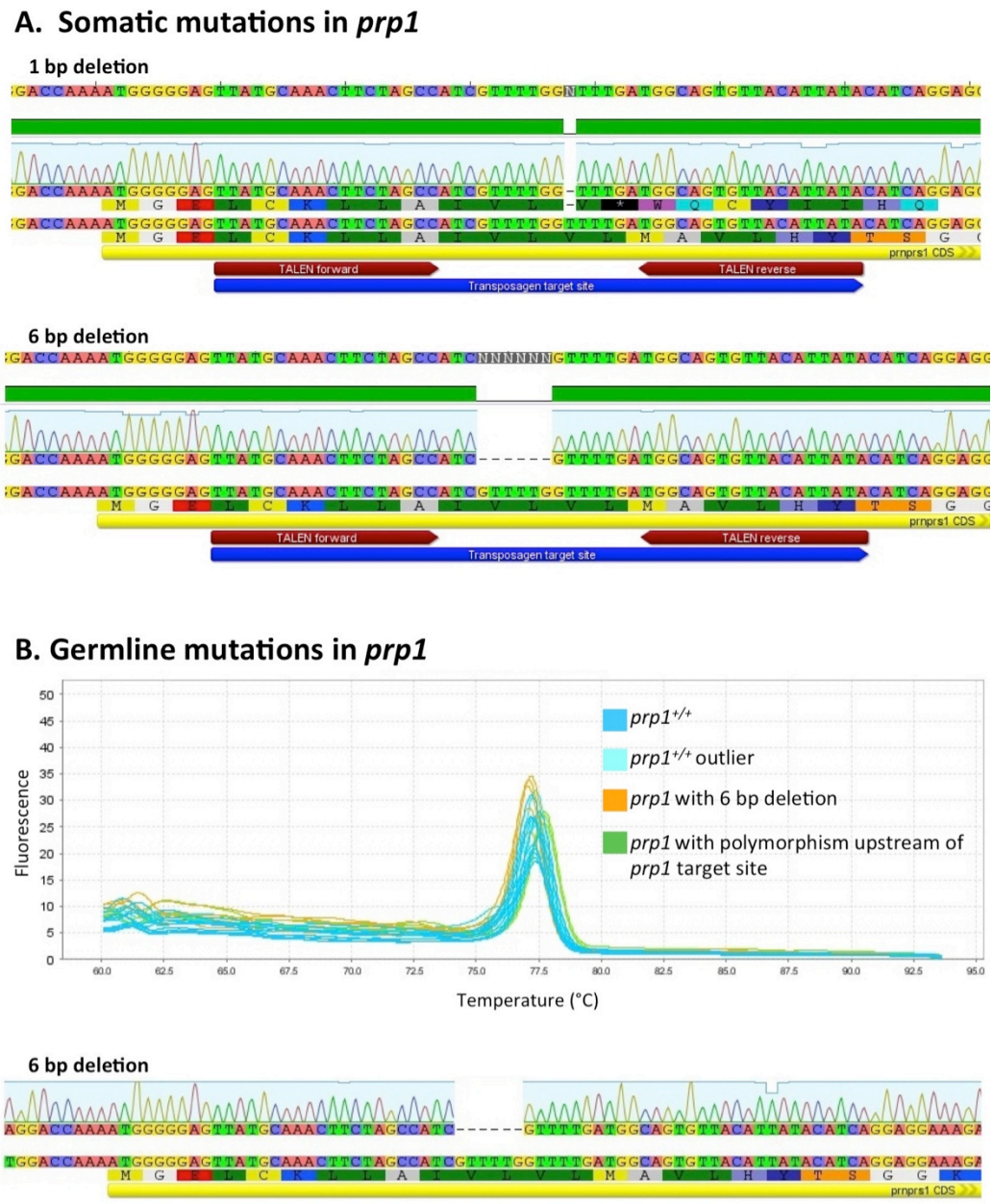

Supplementary Figure S1. We identified somatic in-del mutations in *prp1* TALEN injected embryos and found that TALEN-induced mutations were transmitted through the germline. A. Somatic mutations induced in *prp1* by TALENs. The 1 bp deletion is a frameshift mutation, while the 6 bp deletion is not. **B.** We raised injected (F_0) fish to adulthood and genotyped pools of F_1 generation fish (Topo-clones). This informed us that the F_0 parents were carriers of a 6-bp deletion allele of *prp1*. Unfortunately, in this case the mutation is not predicted to produce a disrupted gene product, as would be expected via frameshift.

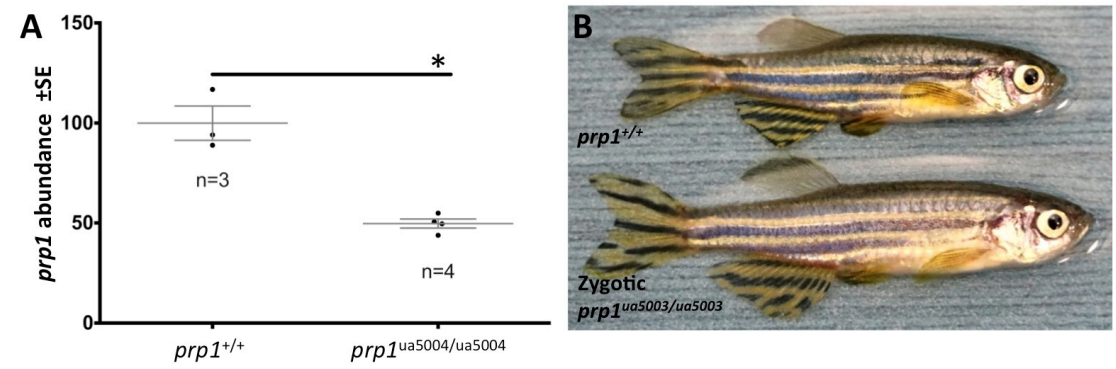

E

Genotype:	Transcript abundance	
	prp1	***prp2***
prp1$^{-/-}$; *prp2*$^{+/+}$	↓	normal
prp1$^{+/+}$; *prp2*$^{-/-}$	normal	↓
prp1$^{-/-}$; *prp2*$^{-/-}$	↓	↓

Supplementary Figure S2. A. *prp1* transcript abundance was reduced by approximately 2-fold in 2dpf *prp1*$^{ua5004/ua5004}$ larvae compared to 2dpf wild type larvae. Here the data is normalized to the wild type fish. *p=0.0012 with the unpaired t-test. n refers to the number of biological replicates (5 larvae/biological replicate). See also Figure 2.. **B.** Zygotic *prp1*$^{ua5003/ua5003}$ adult survive to adulthood and are similar in appearance to adult wild-type fish. **C.** Zygotic *prp1*$^{ua5004/ua5004}$ fish survive to adulthood and have no overt phenotypes compared to wild type fish. **D**. Compound maternal zygotic *prp1*$^{ua5004/ua5004}$;*prp2*$^{ua5001/ua5001}$ zebrafish survive to adulthood and have no overt phenotype compared to wild type fish. **E.** Summary of observations regarding reduced transcript abundance – whenever *prp1* or *prp2* mutants are examined, the cognate transcript (*prp1* or *prp2*) is substantially reduced in abundance.

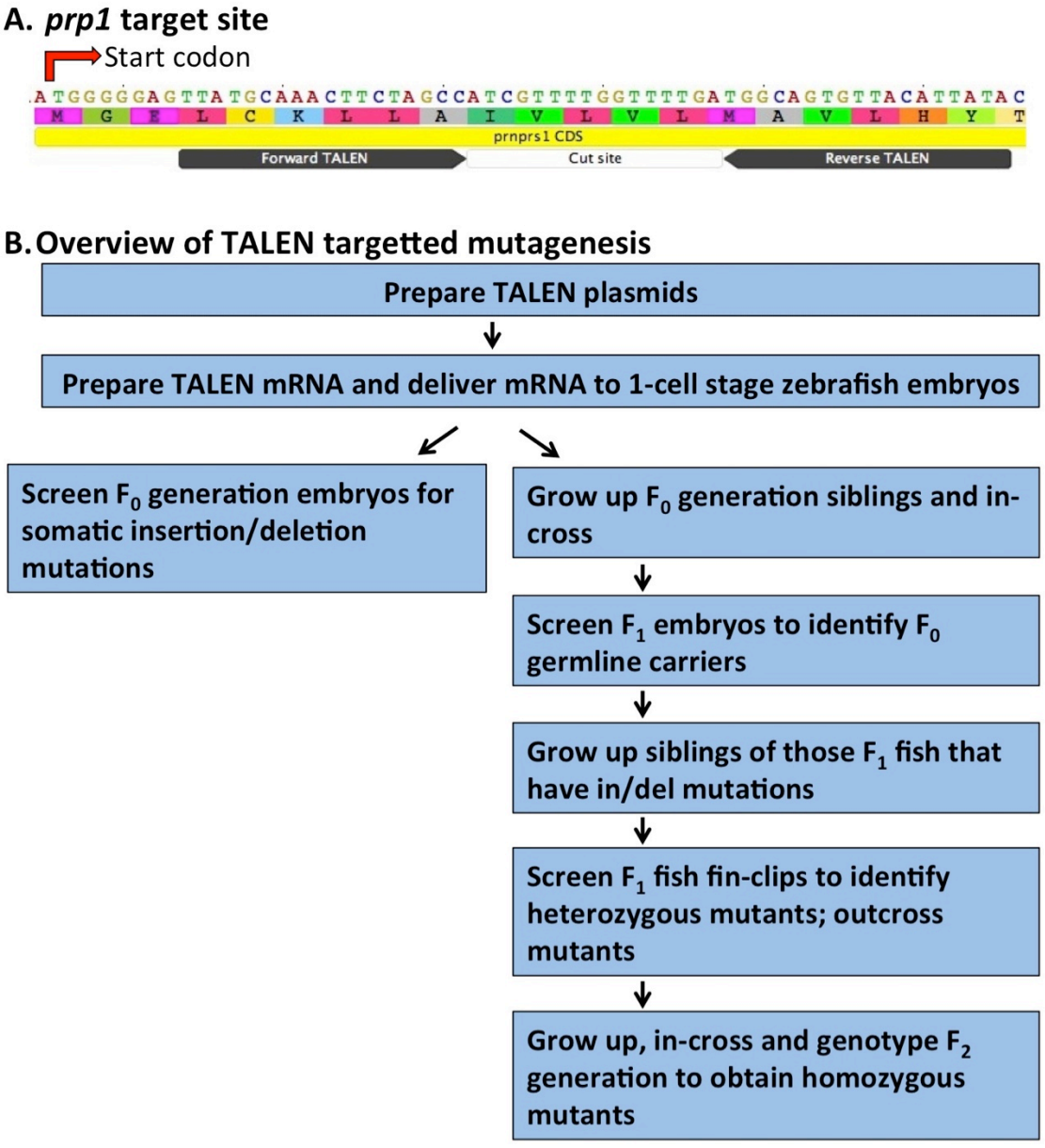

Supplementary Figure S3. The region near the translation start site of *prp1* was targeted using TALENs. A. TALEN forward and reverse binding sites for targetted mutagenesis of *prp1* are shown relative to the translation start site. **B.** Flow-chart detailing the steps undertaken to generate stably inherited loss-of-function *prp1* alleles.

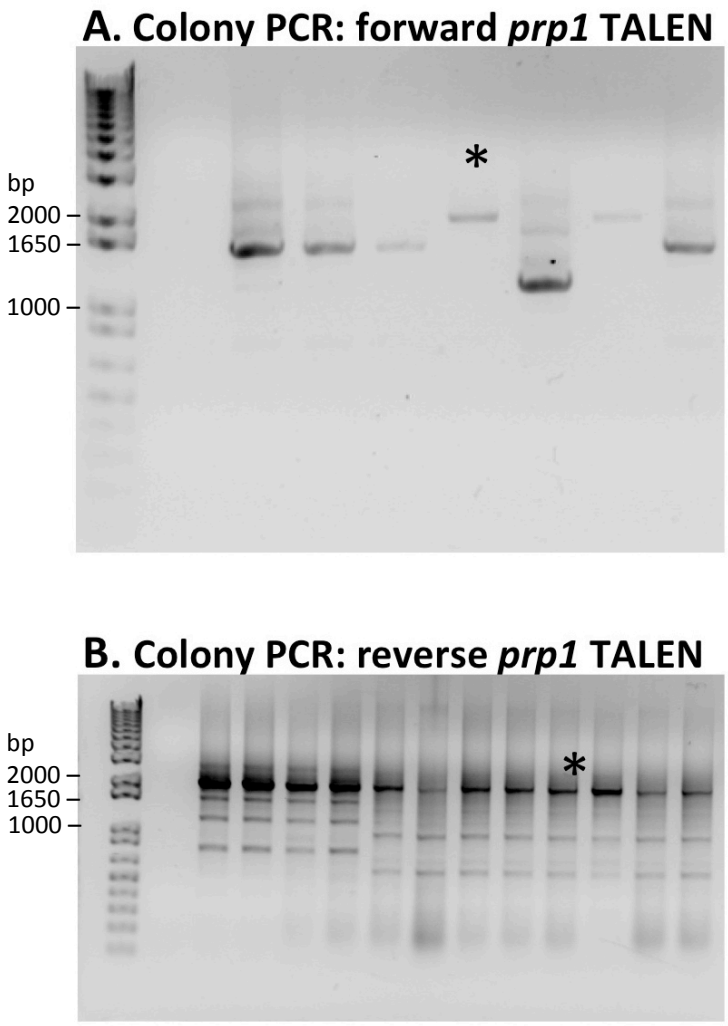

Supplementary Figure S4. Colony PCR for creating TALEN vectors. Constructs containing the correct insert yielded 2.1 kb PCR products. A laddering effect was apparent in most cases because of the repetitive nature of the TALEN nucleotide sequence. **A** *prp1* forward TALEN PCR-products. The construct used to produce the PCR product in lane 6, marked with an asterisk, was sequenced and found to contain the correct insert. **B.** *prp1* reverse TALEN PCR-products. The plasmids that yielded the bands in lane 11 was sequenced and found to contain the correct insert for the *prp1* reverse TALEN.

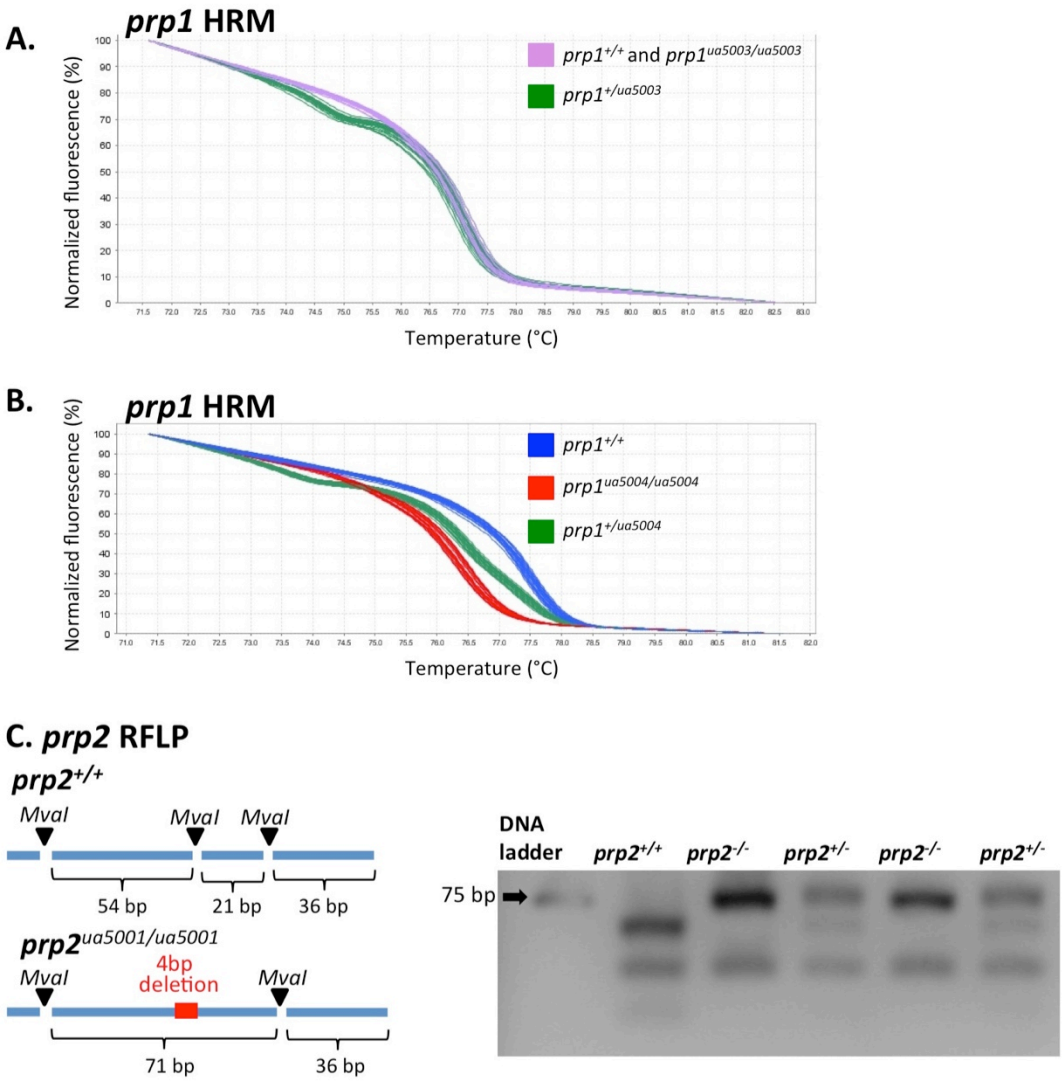

Supplementary Figure S5. Genotyping assays for the *prp1 ua5003* and *ua5004* alleles and the *prp2 ua5001* allele. A. HRM analysis can be used to distinguish *prp1*$^{+/ua5003}$ fish (green curves) from fish that are either *prp1*$^{+/+}$ or *prp1*$^{ua5003/ua5003}$ (magenta curves), but it cannot distinguish the latter two homozygous states. One technical replicate each from three fish was excluded because they did not overlap with the other two replicates. Melt curves from 17 fish (3 technical replicates/fish) are shown here. **B.** *prp1*$^{+/+}$ fish (blue curves), *prp1*$^{+/ua5004}$ (green curves), and *prp1*$^{ua5004/ua5004}$ (red curves) each have unique HRM melt profiles. One technical replicate from one fish was excluded because it did not match the other two replicates. Melt curves from 20 fish (3 technical replicates/fish) are shown here. **C.** Restriction fragment length polymorphism (RFLP) to identify *prp2*$^{+/ua5001}$ and *prp2*$^{ua5001/ua5001}$ fish. Left panel: The restriction enzyme, *MvaI,* cuts the PCR product from a wild type template into 54 base pair (bp), 21 bp and 36 base pair fragments. The *prp2 ua5001* allele lacks one of the *MvaI* cut sites, so 71 bp and 36 bp bands are visible instead. Right panel: Example *prp2* PCR products cut with *MvaI* and separated on an agarose gel.

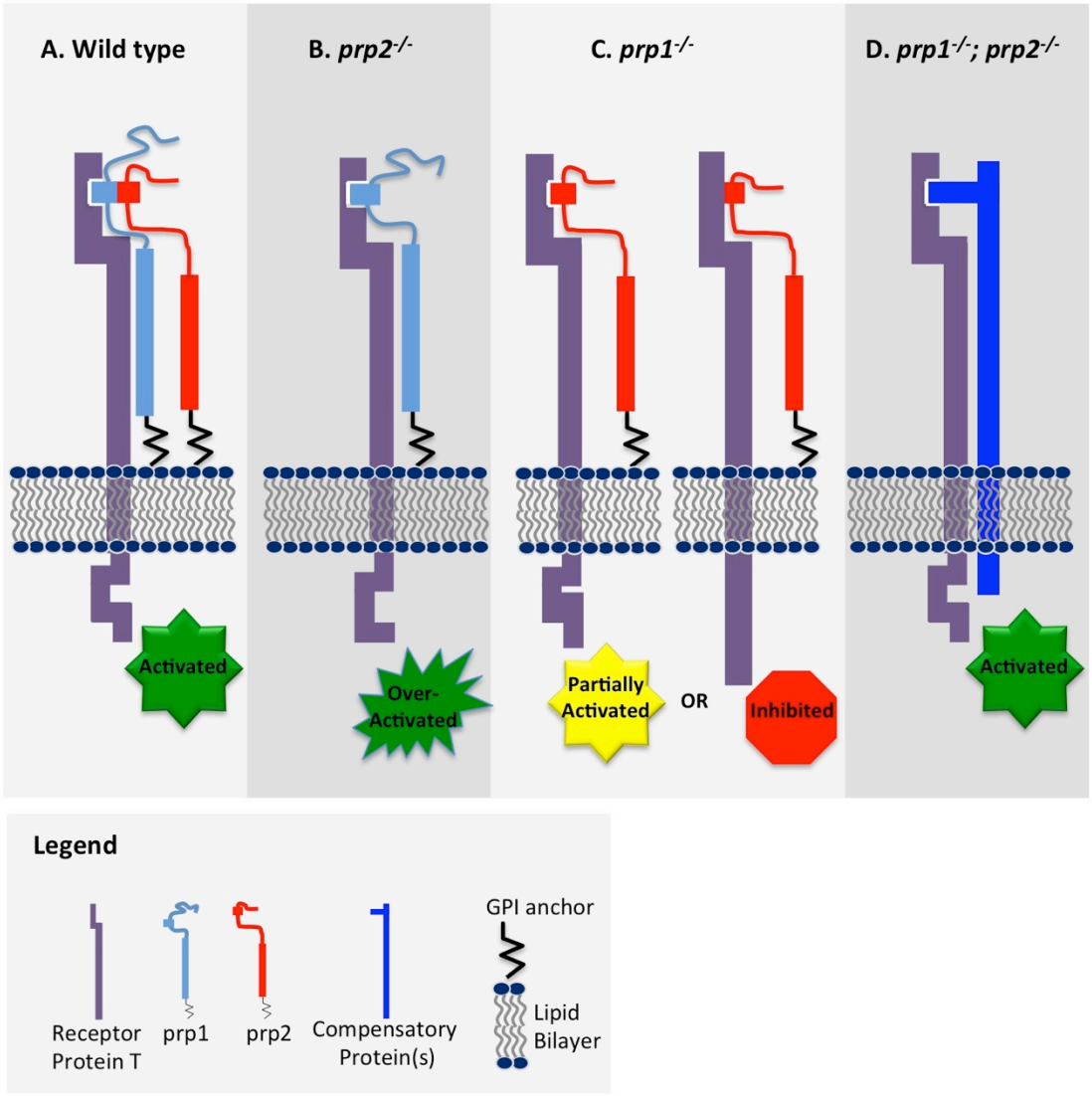

Supplemental Figure S6. Hypothetical model to explain the differential effects of *prp1* and *prp2* loss-of-function on neuromast number and the apparent rescue of both phenotypes in *prp1/prp2* compound mutants. A. Prp1 binds to a membrane receptor, 'Protein T,' thereby activating it in wild type fish. Prp2 regulates this activity by direct binding to Prp1 (shown here) or by competing with Prp1 for access to 'Protein T' (as depicted in panel C). **B.** When Prp2 is absent, Prp1 over-activates 'Protein T'. **C.** When Prp1 is absent, Prp2 outcompetes other substrates for access to 'Protein X'. Prp2 binding to 'Protein T' may reduce or inhibit its normal function. **D.** Absence of Prp1 and Prp2 causes transcription of compensatory genes. Compensatory proteins that may have been present in *prp1*$^{-/-}$ fish can now access 'Protein T' because Prp2 is no longer blocking the receptor-binding site.

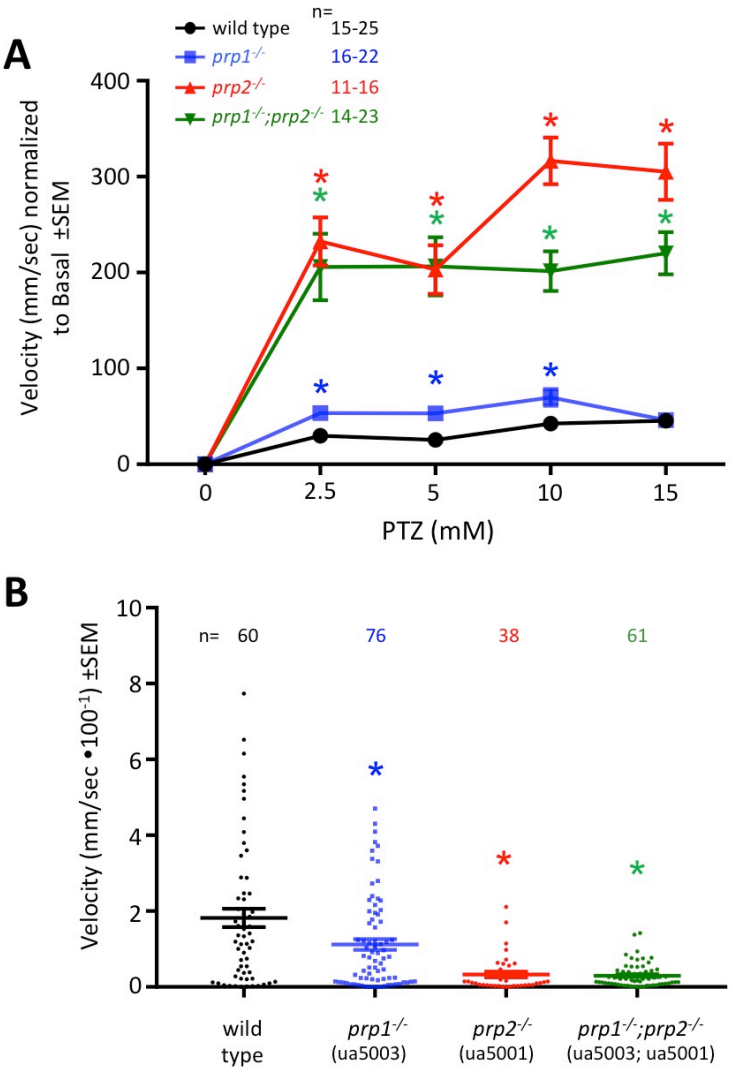

Supplemental Figure S7. Alternative analysis to data in Figure 5 assessing seizures by larval velocity rather than larval activity supports individual roles for both *prp1* and *prp2* in seizure susceptibility, and that those roles are non-additive. The data here (in panels A and B) are the same behavioural traces as those analyzed in Figure 5 (panels C and D), except that only a subset met the criteria to be analyzed by velocity. In principal, assessing seizures by different metrics can suggest different interpretations; in this case, the data derives the same broad conclusions (in the title of this Figure Legend) regardless of video analysis method. Assessing the videos of seizure activity by velocity was more challenging in this data set, as it requires the video tracking software correctly identifies the position of the larva with good fidelity throughout thousands of frames of video (tracking activity does not suffer from this, as it uses a frame-to-frame comparison of which pixels are changing in intensity), explaining the reduced sample size here compared to Figure 5. Symbol * indicates statistically significant compared to wild type at $p<0.05$, and outlier data were removed objectively in Prism software at ROUT Q=0.1. See also Supplemental Figure S8 which repeats this type of analysis with video and arenas optimized for quantifying seizures via additional assays.

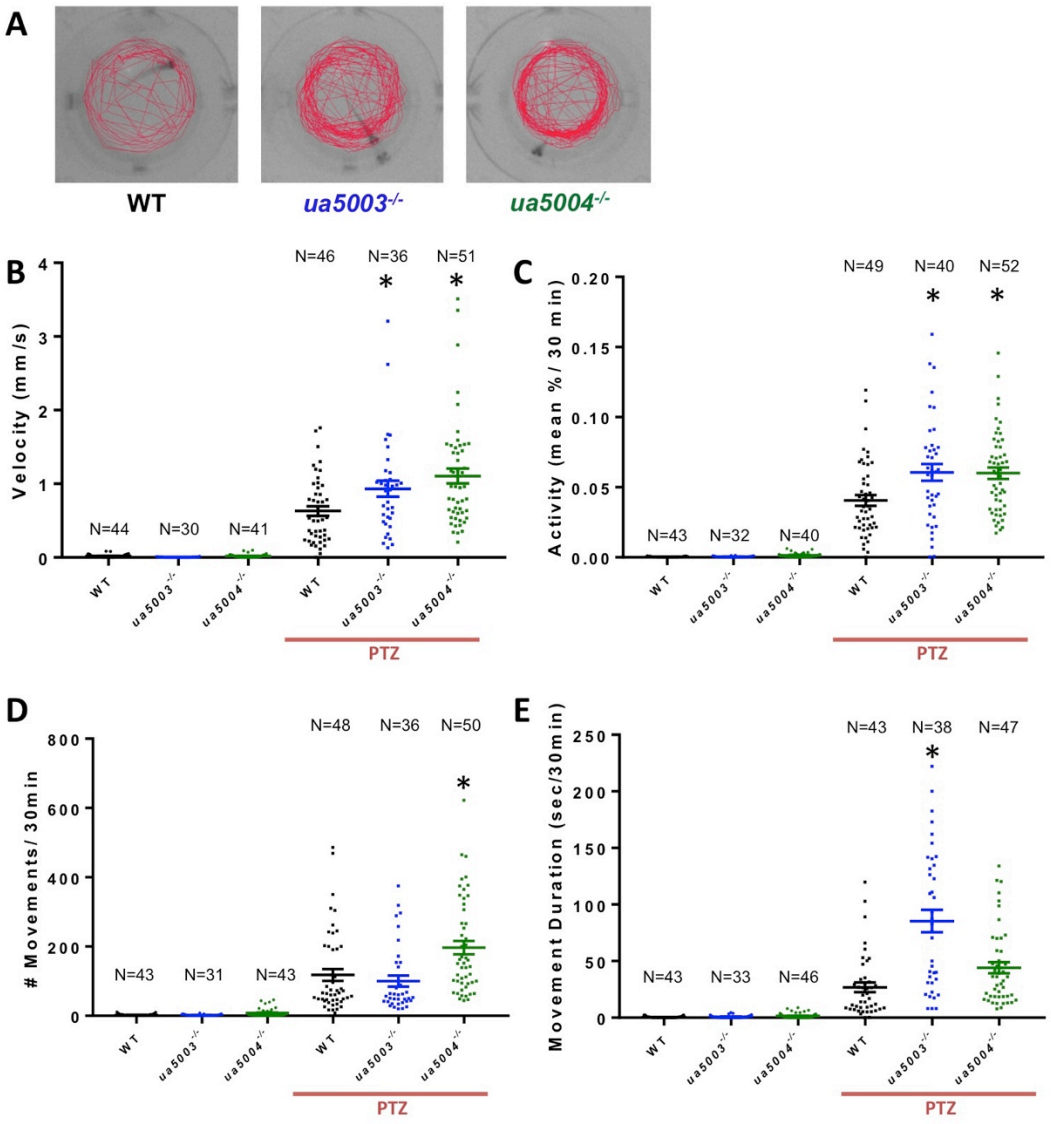

Supplemental Figure S8. Quantifying seizure activity, similar to Figure 5, confirms seizure susceptibility in prion mutant fish by using different clutches of larvae, different equipment, different outputs and a second *prp1* mutant allele. Using a different equipment configuration compared to data in Figure 5 (improved optics and round arenas), the seizure activity of larvae was able to be assessed with additional parameters. **A.** Traces of typical zebrafish movement during following addition of convulsant pentylenetetrazol (PTZ). Note round activity arenas in 96 well plate, as opposed to square arenas in Figure 5. **B-E.** All four panels of data are different analyses of the same behavioural tracking data, affirming that the phenotype is not an artefact of the methods used. PTZ applied at 5 mM increased velocity and activity of *prp1* mutants significantly more than observed in wildtype larvae. The increase in the mean convulsant-induced velocity and activity were similar in two independent alleles of *prp1* mutants, ua5003 and ua5004. Symbol * indicates statistically significant compared to wild type with PTZ at $p<0.05$, and outlier data were removed objectively in Prism software at ROUT Q=0.1.

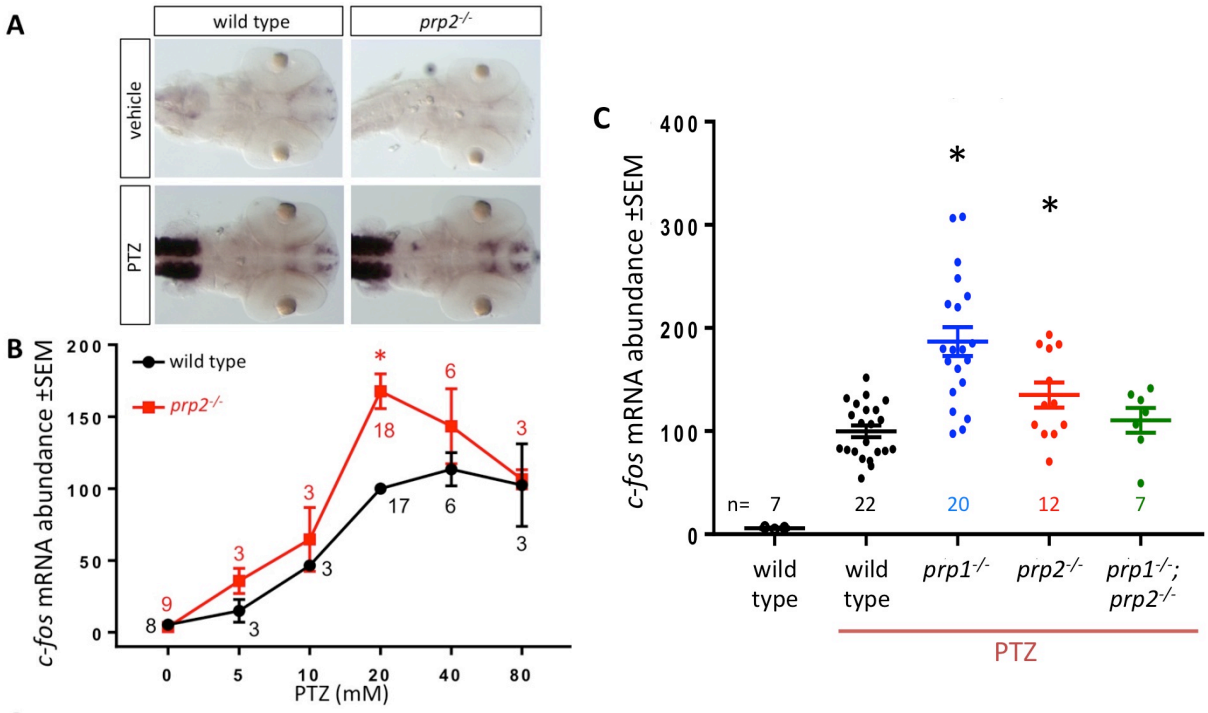

Supplemental Figure S9. Quantifying seizure susceptibility, associated with Figure 5, by measuring abundance of the immediate early gene *c-fos*, confirms prion mutant zebrafish have increased susceptibility to convulsant, and these phenotypes in *prp1* and *prp2* mutants are not additive. Abundance of *c-fos* is a metric of neural activity. Larvae were treated with convulsant pentylenetetrazol (PTZ), representing independent clutches of larvae compared to those assessed by swimming activity, and assessed for *c-fos* abundance using *in situ* hybridization and/or RT-qPCR. **A.** Abundance of immediate early gene *c-fos* increases following treatment with PTZ, and increases more in *prp2*$^{-/-}$ mutants. Dorsal view of larvae *c-fos* detection with *in situ* hybridization (purple). **B.** RT-qPCR analysis of *c-fos* mRNA in zebrafish (2 dpf) compared between wildtype (WT; black) or *prp1*$^{ua5001/ua5001}$ (*prp2*$^{-/-}$; red) with varying PTZ concentrations (90 min of treatment). Data was normalized to the endogenous control gene *β-actin*. Quantity presented relative to the average *c-fos* abundance in WT with 20 mM PTZ. The number of biological replicates (n) are shown beside the data points in corresponding colors. * Statistically significant compared to wild type ($p<0.05$, two-tailed ANOVA with Holms-Sidak). **C.** Various prion mutant zebrafish larvae were treated with PTZ (20 mM) for 90 min. *wt*, *prp1*$^{ua5004/ua5004}$ (*prp1*$^{-/-}$), *prp2*$^{ua5001/ua5001}$ (*prp2*$^{-/-}$), and compound mutant for *prp1*$^{ua5003/ua5003}$;*prp2*$^{ua5001/ua5001}$ (*prp1*$^{-/-}$;*prp2*$^{-/-}$) were treated at 3 dpf. Raw data obtained from 3 dpf larvae was combined and normalized *c-fos* expression levels were presented as % in comparison to wildtype treated with PTZ. Lines represents the mean ± SEM. * Statistically significant ($p<0.05$) compared to WT + PTZ via one-way ANOVA and Dunnett's Multiple Comparison. The number of biological replicates (n) are shown below the data points in corresponding colors.

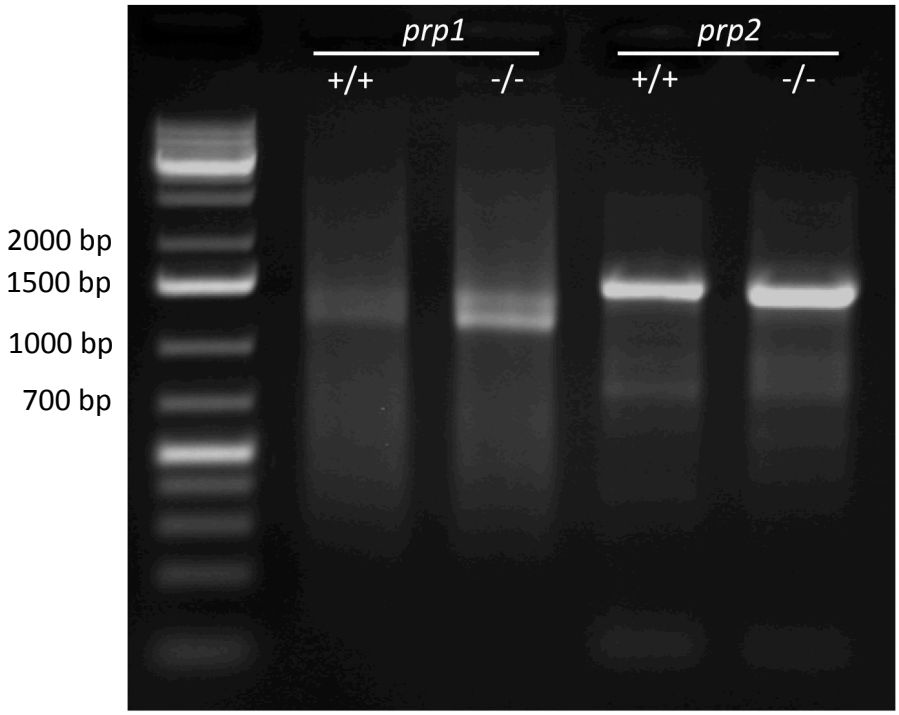

Supplemental Figure S10. Supplemental Figure S10. Characterizing mutant transcripts by RACE PCR. Random amplification of cDNA Ends (RACE) was used to look for abnormal transcript structure at the 5' end of *prp1* and *prp2* mutant transcripts. For both *prp1* and *prp2* transcripts, the sizes of each were indistinguishable between mutant and wild type samples, as confirmed by sequencing.

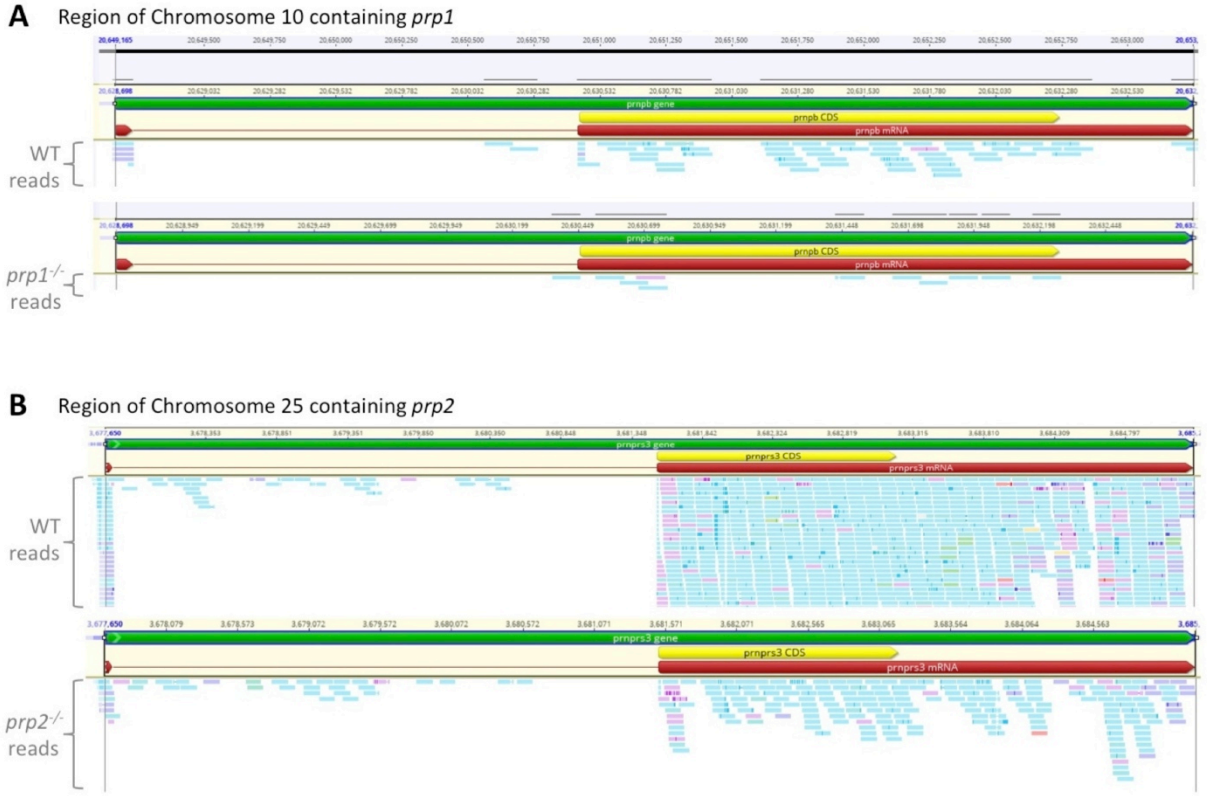

Supplemental Figure S11. Characterizing mutant transcripts by examining reads from RNA-Seq. To assess if the mutant *prp1* or *prp2* transcripts produce oddities in their exons, we examined the alignment of RNA Sequencing reads at each gene locus and compared the position of reads when RNA was extracted from wild type (WT) vs. *prp1*$^{-/-}$;*prp2*$^{-/-}$ larvae at 3dpf. In both genes, and as in mammals, the coding region (yellow Coding DNA Sequence, CDS) of the gene is contained within a single exon. The exons of each gene are represented in red. The position of the reads (in eggshell blue or other similar pastel colours) and are typically below the CDS and do not substantially differ based on genotype; i.e. there is no detectable signal of oddly spliced transcript in the *prp1*$^{-/-}$;*prp2*$^{-/-}$ larvae. **A.** Alignment of RNA sequencing reads to the region of zebrafish chromosome 10 that contains the *prp1* gene. Top half of figure shows reads from wild type larvae, and bottom half dispays the reads from *prp1*$^{-/-}$;*prp2*$^{-/-}$ larvae. Note that by 3 days old zebrafish have a very low abundance of *prp1* transcripts, and the *prp1* mutants have a dramatic reduction below this (~5 fold). **B.** Alignment of RNA sequencing reads to the region of zebrafish chromosome 25 that contains the *prp2* gene. Top half shows abundant *prp2* reads that extend below the frame of the figure as presented, especially abundant below each exon. This contrasts the abundance of *prp2* transcript in *prp1*$^{-/-}$;*prp2*$^{-/-}$ larvae (bottom half), where the number of reads is substantially reduced (~10-fold).

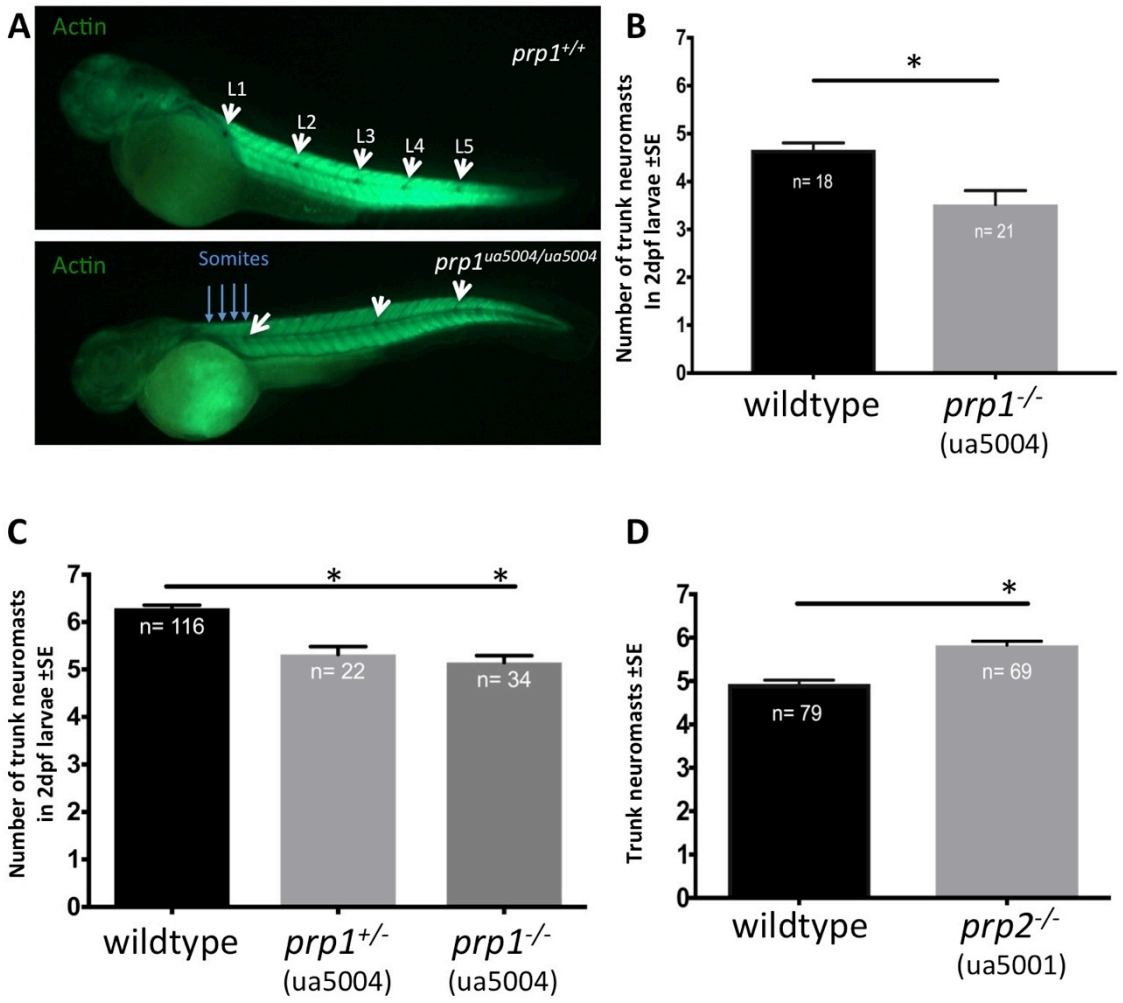

Supplemental Figure S12. Neuromast abundance is modulated by prion genes in a non-additive fashion. A. 2dpf wild type AB strain (*prp1*$^{+/+}$) zebrafish larvae (top) has 5 trunk neuromasts, while a 2 dpf maternal zygotic *prp1*$^{ua5004/ua5004}$ larvae (bottom) has 3 trunk neuromasts. Neuromasts are visualized by endogenous alkaline phosphatase labeling and larvae are counterstained with phalloidin 488. **B.** Quantification of the number of neuromasts through labeling of endogenous alkaline phosphatase revealed a reduction in trunk neuromast number in maternal zygotic *prp1*$^{ua5004/ua5004}$ mutants compared to wild type (*prp1*$^{+/+}$) fish. *p<0.05 with Mann Whitney U test. **C**. Quantification of the number of neuromasts in fish revealed a reduction in trunk neuromast number in both 2 dpf *prp1*$^{+/ua5004}$ fish and 2 dpf maternal zygotic *prp1*$^{ua5004/ua5004}$ fish compared to 2dpf cldnb:gfp *prp1*$^{+/+}$ larvae. *p<0.05 with one-way ANOVA. **D.** Quantification of the number of trunk prim I neuromasts in in 3dpf larvae revealed an increase in neuromast number in maternal zygotic *prp2*$^{ua5001/ua5001}$ mutants compared to wild type AB strain larvae. Both groups include offspring from 4 sets of parents (4 clutches/genotype). *p<0.0001 with unpaired t-test. Sample sizes (n=) refers to the number of fish. Raw data for panels B to D appear in Supplemental Tables S5 to S7, respectively.

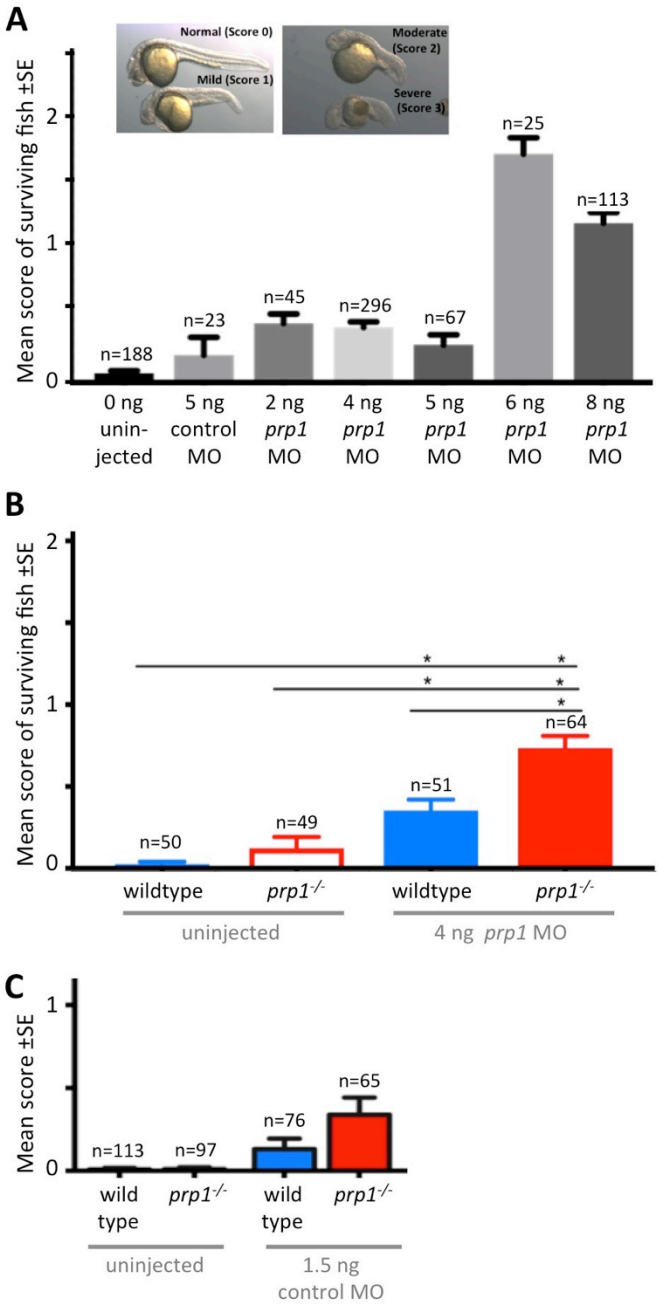

Supplemental Figure S13. High doses of morpholino directed against *prp1* cause phenotypes in *prp1* mutant animals. A test of morpholino (MO) specificity is to assess if it produces a phenotype in animals with mutations in the cognate target gene. Therefore if *prp1* MO is specific at a particular dose, it is predicted to not induce a phenotype in *prp1* mutants. **A.** Delivery of *prp1* MO into **wildtype** embryos, at doses higher than we have used in the past (Kaiser *et al* 2012), produced defects in development (inset shows scoring of phenotypes). **B.** delivery of *prp1* MO at these high doses demonstrated that its impacts on development were not reduced in *prp1* mutants. Indeed the phenotypes were more severe in *prp1* mutants, however this may reflect a sensitivity of *prp1* mutants to general MO injection, because a standard control MO also caused more phenotypes in *prp1* mutants (**C**).